

The thermal expansion of staurolite, $\text{Fe}_4\text{Al}_{18}\text{Si}_8\text{O}_{44}(\text{OH})_4$

K. GIBBONS, M. J. DEMPSEY, AND C. M. B. HENDERSON

Department of Geology, University of Manchester, Manchester M13 9PL, England

ABSTRACT. The thermal expansion of iron end-member staurolite has been studied by high-temperature powder X-ray diffraction methods and by modelling with the Distance Least Squares (DLS) computer program. The X-ray approach was complicated by dehydroxylation of the staurolite. Mean linear expansion coefficients for the *a*, *b*, and *c* cell edges of dehydroxylated staurolite determined by the X-ray method are ($\times 10^{-6} \text{ }^\circ\text{C}^{-1}$): 20–500 $^\circ\text{C}$, 8.93, 8.23, and 7.95, respectively, and 20–800 $^\circ\text{C}$, 7.85, 9.43, and 9.13, respectively. Expansion coefficients of *a*, *b*, and *c* calculated for hydroxylated staurolite using the DLS program over the same temperature ranges are (7.86 , 7.18 , and $7.55 \times 10^{-6} \text{ }^\circ\text{C}^{-1}$) and (7.87 , 7.17 , and $7.57 \times 10^{-6} \text{ }^\circ\text{C}^{-1}$). The good agreement between the results from the two methods supports the use of computer modelling in estimating the thermal expansion behaviour of complex structures. The latter approach could be preferable for studying hydrated minerals.

As part of a study on the stability relations and thermodynamic properties of iron end-member staurolite, $\text{Fe}_4\text{Al}_{18}\text{Si}_8\text{O}_{44}(\text{OH})_4$, one of us (K. G.) found that although compressibility data exist for this mineral (Birch, 1966) thermal expansion data are not available. We decided to rectify this deficiency and have used two independent methods: an experimental study of a synthetic iron staurolite, and a computer simulation using the Distance Least Squares (DLS) program originally developed by Meier and Villiger (1969) at ETH Zurich and modified by Dempsey and Strens (1976).

The interpretation of the results from the X-ray study were complicated by the dehydroxylation of the staurolite at about 500 $^\circ\text{C}$. This problem was avoided in the computer simulation method and hence high-temperature data for the hydroxylated structure were obtained.

Experimental techniques. A gel of composition $\text{Fe}_4\text{Al}_{18}\text{Si}_8\text{O}_{46}$ was prepared using the method described by Hamilton and Henderson (1968). The iron in the gel, which oxidized to Fe^{3+} during the gel preparation, was reduced to Fe^{2+} in a gas mixing furnace. The reduced gel was then sealed in a gold capsule with 10 wt% water and run in a conventional piston-cylinder apparatus at 19 kb

and 710 $^\circ\text{C}$ for 14 hours. The run products were checked by X-ray diffraction and found to consist of staurolite plus quartz. Richardson (1966) also reported the presence of quartz in his synthesis of staurolite from similar bulk compositions to ours. Electron-microprobe analysis of our synthetic staurolite gave an average formula unit of $\text{Fe}_{4.15(\pm 0.08)}\text{Al}_{18.18(\pm 0.18)}\text{Si}_{7.28(\pm 0.14)}\text{O}_{48}\text{H}_4$, assuming that only Fe^{2+} is present and that there are four hydrogen atoms per formula unit as suggested by Smith (1968). This composition is similar to that deduced for synthetic Fe staurolite by Richardson (1966; i.e. $\text{Fe}_4\text{Al}_{18}\text{Si}_{7.5}\text{O}_{48}\text{H}_4$). The presence of quartz in the synthetic products is clearly related to the SiO_2 -deficiency in the staurolite.

The thermal expansion of the synthetic staurolite was determined by the method of Henderson and Taylor (1975) in which peaks from the platinum sample holder are used for internal standardization. Cell parameters were calculated by least squares, assuming orthorhombic symmetry ($\beta = 90^\circ$), using at least 12 peaks from 040, 220, 201, 150, 221, 002, 060, 151, 241, 132, 330, 311, 202, 171, and 062. Cobalt radiation was used with $\text{Co-}K\alpha = 1.79021 \text{ \AA}$ and $\text{Co-}K\alpha_1 = 1.78892 \text{ \AA}$ and the platinum plate was calibrated at room temperature with Si ($a = 5.4307 \text{ \AA}$).

Infra-red spectra were obtained for hydroxylated and dehydroxylated synthetic staurolite and hydroxylated natural staurolite using KBr discs (1 mg sample in 150 mg KBr) and a Perkin-Elmer 577 spectrophotometer.

Experimental results. The room-temperature cell volume for unheated synthetic staurolite (745 \AA^3 , Table I) is larger than the volumes reported for natural staurolites ($739\text{--}41 \text{ \AA}^3$; Griffen and Ribbe, 1973) and this is presumably related to the higher Fe and Al contents of the synthetic sample. Infra-red spectra show that the area under the OH-stretching band at $\sim 3440 \text{ cm}^{-1}$ (Hanisch, 1966) is about 40% greater in unheated synthetic staurolite than in natural staurolite. This supports the

suggestion (Smith, 1968) that synthetic specimens may contain more OH groups than natural staurolites because of the high water pressure of the synthesis. Thus the deficiency of Si in synthetic staurolite (see above) could be the result of the presence of excess protons.

The first series of measurements, denoted Run 1, were carried out at temperatures to 790 °C but the cell parameters at room temperature after these experiments are significantly different from the original values (Table I); the sample clearly suffered an irreversible change during Run 1. A second series of measurements with the same sample, denoted Run 2 (Table I), were carried out up to 860 °C. Cell parameters at room temperature after 450 °C and after 860 °C are essentially the same as the values at the start of Run 2 (Table I) indicating that no further change occurred in the sample during these experiments. The infra-red spectrum for the sample after Run 2 does not show any absorption band for OH, thus the sample must have been completely dehydroxylated during Run 1. After the dehydroxylation the staurolite X-ray diffraction peaks were as sharp as in the unheated sample and no extra peaks were observed; thus the staurolite did not break down during dehydroxylation.

As a result of the dehydroxylation reaction during Run 1 the room-temperature *a* and *b* parameters show small increases while the *c* parameter shows a large decrease (~ 0.04 Å, Table I). A possible explanation for this behaviour may be found in the location of the hydrogen atoms in the crystal structure. Takeuchi *et al.* (1973) proposed that the H atoms are located within the Al(3A) and Al(3B) octahedra which form chains parallel to *c*. During dehydroxylation, bonds within these octahedra would be broken causing a weakening of the structure and leading to collapse along *c*.

The measured thermal expansion curves are illustrated in fig. 1. The changes in the rate of expansion at 400–500 °C in the curves for Run 1 clearly reflect the onset of the dehydroxylation reaction. The very broad and ragged 002 reflection in the X-ray chart at 600 °C suggests that much of the dehydroxylation took place during this experiment. Thus the dashed curves (drawn by eye) through the lower temperature points for Run 1 are assumed to represent the expansion of the synthetic staurolite prior to dehydroxylation. The higher-temperature cell parameters for Run 1 are not reliable because of incomplete dehydroxylation effects, especially on *c*.

The expansion curves for Run 2 (fig. 1) represent the expansion of dehydroxylated synthetic staurolite. These curves were fitted to a second-order polynomial using linear regression and the result-

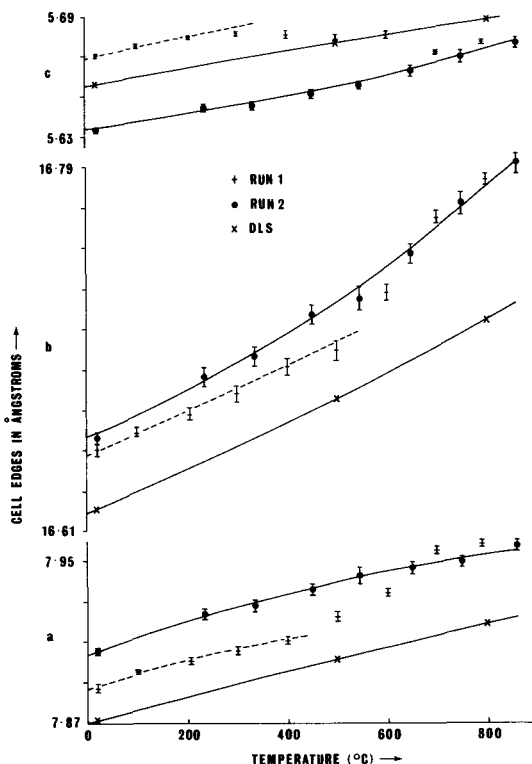


FIG. 1. Observed and calculated cell edges of staurolite as a function of temperature. The error bars represent one standard deviation.

ing regression coefficients together with mean thermal expansion coefficients are given in Table I.

The DLS method. The Distance Least Squares method uses the fact that in most structures the number of crystallographically independent interatomic distances exceeds the number of variables (atomic coordinates and cell parameters) to be determined. Consequently, the latter may be calculated by specifying a sufficient number of the former. By adjusting the variables from approximate initial values the DLS program minimizes the function:

$$S = \sum_j [w_j(D_j^o - D_j^c)]^2$$

where D_j^o is the *j*th prescribed (input) distance, D_j^c the corresponding calculated distance, and w_j is the weight given to the *j*th distance. The sum is over the inequivalent distances in the structure.

The weighting scheme used was that developed by Dempsey and Strens (1976). This gives weights equal to the bond strengths (in valence units) of the metal–oxygen distances. These bond

strengths can be derived either from the bond-length-bond strength relations of Brown and Shannon (1973) or those of Brown and Wu (1976). In this study the latter were used. The constants used to calculate the metal-oxygen weights are given in Table II along with the metal-oxygen bond thermal expansion coefficients from Cameron *et al.* (1973). The latter were used to calculate the high temperature prescribed (input) distances for the program. The corresponding oxygen-oxygen prescribed distances were calculated by assuming that their expansion was proportional to that of the appropriate metal-oxygen distances.

The structural refinement of staurolite by Smith (1968) was used as a basis for the atomic coordinates and interatomic distances used by the program. In preparing the structural data several assumptions were made: hydrogen atoms were located at $(0, 0, \frac{1}{2})$ and $(\frac{1}{2}, \frac{1}{2}, \frac{1}{2})$ in Smith's Al(3B) sites; all of the Fe^{2+} was in tetrahedral coordination; the symmetry of the staurolite structure was monoclinic with $\alpha = \gamma = 90^\circ$ and $\beta \approx 90^\circ$.

As a check on the input data the program was first run with Smith's interatomic distances and approximate values of atomic coordinates and cell parameters. The results from this were satisfactory

Table I Experimental cell parameters, linear regression coefficients and thermal expansion coefficients for synthetic Fe staurolite

Cell parameters for Run 1				
T ^o C	a(Å)	b(Å)	c(Å)	V(Å ³)
20	7.888(2)*	16.650(3)	5.670(1)	744.7(2)
20 (after 790)	7.905(3)	16.658(4)	5.634(2)	741.9(3)
100	7.895(1)	16.659(2)	5.675(1)	746.3(1)
205	7.900(2)	16.668(3)	5.679(1)	747.7(2)
300	7.905(2)	16.677(4)	5.681(1)	749.0(2)
400	7.910(2)	16.691(4)	5.681(2)	750.1(3)
500	7.922(3)	16.699(5)	5.679(2)	751.2(3)
600	7.934(2)	16.728(4)	5.681(2)	754.0(3)
700	7.955(2)	16.765(3)	5.672(1)	756.4(2)
790	7.958(2)	16.784(3)	5.677(1)	758.2(2)

Cell parameters for Run 2

T ^o C	a(Å)	b(Å)	c(Å)	V(Å ³)
20 (after Run 1)	7.905(3)	16.658(4)	5.633(2)	741.9(3)
20 (after 450)	7.907(2)	16.657(3)	5.635(1)	742.1(2)
20 (after 860)	7.903(2)	16.656(5)	5.631(2)	741.3(3)
235	7.924(3)	16.687(5)	5.645(2)	746.4(4)
335	7.927(3)	16.696(5)	5.646(2)	747.3(4)
450	7.936(3)	16.717(5)	5.652(2)	749.8(4)
545	7.943(4)	16.725(6)	5.656(2)	751.4(4)
650	7.946(3)	16.748(5)	5.663(3)	753.7(3)
750	7.949(3)	16.772(6)	5.671(3)	756.1(4)
860	7.957(3)	16.792(5)	5.678(3)	758.6(4)

Linear regression coefficients for Run 2**

x	7.9037	16.6565	5.6336	741.8
y	8.355×10^{-5}	9.720×10^{-5}	3.049×10^{-5}	1.570×10^{-2}
z	-2.705×10^{-8}	7.065×10^{-8}	2.411×10^{-8}	4.306×10^{-6}

Mean thermal expansion coefficients for Run 2. (Units $\times 10^{-6} \text{ }^\circ\text{C}^{-1}$)

α_{20-500}^{***}	8.93	8.23	7.95	24.71
α_{20-800}	7.85	9.43	9.13	26.27

* Figures in parentheses are the e.s.d.'s in terms of the least units cited.

** Cell edges fitted to the polynomial: cell edge = $x + yT + zT^2$.

*** $\alpha_{20-T} = \frac{1}{a_{20}} \left(\frac{a_T - a_{20}}{T - 20} \right)$

Table II Constants used in DLS calculations

	CN	r _o	N	α (Units $\times 10^{-6} \text{ }^\circ\text{C}^{-1}$)
Si-O	4	1.622	4.29	1.92
Fe ²⁺ -O	4	1.764	5.5	7.81
Al-O	6	1.622	4.29	10.02
H-O	1	0.87	2.2	-

CN = coordination number

r_o, N = parameters used in Brown and Wu's (1976) bond length-bond strength relation, $s = (r_o/r)^N$, where s is the bond strength of a bond of length r.

α = observed metal-oxygen expansion coefficients from Cameron *et al.* (1973).

Table III Calculated DLS cell parameters and thermal expansion coefficients

T ^o C	a(Å)	b(Å)	c(Å)
20*	7.8713	16.6204	5.6560
500	7.9010	16.6777	5.6765
800	7.9196	16.7133	5.6894

Thermal expansion coefficients (Units $\times 10^{-6} \text{ }^\circ\text{C}^{-1}$)

α_{20-500}	7.86	7.18	7.55
α_{20-800}	7.87	7.17	7.57

* The 20°C cell parameters are those of Smith (1968)

and so the program was then run with the calculated prescribed interatomic distances for 500 and 800 °C. The resulting cell parameters and the thermal expansion coefficients calculated from them are given in Table III. The cell parameters are also plotted along with the thermal expansion data in fig. 1. The complete set of high-temperature structural data can be obtained from the authors.

Discussion. A comparison of the calculated (DLS) and experimental expansion curves (Run 2), in fig. 1, shows that there is good agreement between the behaviour of the model and the X-ray measurements. The thermal expansion coefficients, up to 500 °C, determined from the two methods lie within ~ 10% of each other. It is also interesting to note that in Run 1 the thermal expansion curve lies parallel to the other two curves up to the onset of significant dehydroxylation. This means that the dehydroxylated and hydroxylated structures are behaving in a similar manner up to about 500 °C. Above 500 °C the DLS values represent the expansion of a hydroxylated structure and discrepancies between these and the Run 2 values (dehydroxylated staurolite) become more apparent, particularly in the expansion of *b*.

Because of the complexities introduced by dehydroxylation of the sample during the experimental measurements, we recommend that the best estimates for the thermal expansion behaviour of staurolite are given by the DLS values.

The relatively good agreement between the results of the two methods is encouraging for the further use of computer modelling as a method for determining the expansion behaviour of other complex structures and this approach should be particularly valuable for investigating hydrated minerals.

Acknowledgements. We thank Dr D. Taylor for his comments on an earlier version of this paper. The work was supported by a research grant for Experimental Petrology and Mineralogy awarded by the Natural Environment Research Council. K. G. was supported by the Boyd-Dawkins Fund of the University of Manchester. We would also like to thank Dr Ch. Baerlocher of ETH Zurich for kindly providing a copy of the DLS-76 program.

REFERENCES

- Birch, F. (1966). *Mem. Geol. Soc. Am.* **97**, 107-73.
 Brown, I. D., and Shannon, R. D. (1973). *Acta Crystallogr.* **A29**, 266-82.
 — and Wu, D. K. (1976). *Ibid.* **B32**, 1957-9.
 Cameron, M., Sueno, S., Prewitt, C. T., and Papike, J. J. (1973). *Am. Mineral.* **58**, 594-618.
 Dempsey, M. J., and Strens, R. G. J. (1976). *Physics and chemistry of minerals and rocks* (R. G. J. Strens, ed., Wiley), 443-58.
 Griffen, D. T., and Ribbe, P. H. (1973). *Am. J. Sci.* (Cooper Volume), **273-A**, 479-95.
 Hamilton, D. L., and Henderson, C. M. B. (1968). *Mineral. Mag.* **36**, 832-38.
 Hanisch, K. (1966). *Neues Jahrb. Mineral., Monatsh.* 362-6.
 Henderson, C. M. B., and Taylor, D. (1975). *Trans. J. Brit. Ceram. Soc.* **74**, 55-7.
 Meier, W. M., and Villiger, H. (1969). *Z. Kristallogr.* **129**, 411-23.
 Richardson, S. W. (1966). *Ann. Rept. Dir. Geophys. Lab.* **65**, 248-52.
 Smith, J. V. (1968). *Am. Mineral.* **53**, 1139-55.
 Takeuchi, Y., Aikawa, N., and Yamamoto, T. (1972). *Z. Kristallogr.* **136**, 1-22.

[Manuscript received 13 June 1980;
 revised 28 July 1980]